3910 J. Phys. Chem. A 2004, 108, 3910−3915

A Cluster Study of Cl_2^- Microhydration: Size-Dependent Competition between Symmetrical H-Bonding to the Anion and the Formation of Cyclic Water Networks in the $Cl_2^-\cdot 1-5(H_2O)$ Series

Erica A. Price, Nathan I. Hammer, and Mark A. Johnson*

Sterling Chemistry Laboratory, Yale University, P.O. Box 208107, New Haven, Connecticut 06520

Received: November 11, 2003; In Final Form: January 30, 2004

We report argon predissociation spectra of the $Cl_2^-\cdot nH_2O$ ($n = 1-5$) clusters in the OH stretching region. The spectra of the mono- and dihydrates consist of only a single sharp feature, indicating that the water molecules bind symmetrically to the ion in both cases. The spectra become much more complex in the $n = 3-5$ clusters, displaying band positions consistent with the formation of cyclic networks similar to those found in the hydration of other small diatomic anions. We contrast this behavior with that of the related $Cl^-\cdot(H_2O)_{1-3}$ clusters, where the primary difference arises from delocalization of the excess electron density over two atomic centers in the diatomic anion.

I. Introduction

Recent advances in size-selected infrared spectroscopy,[1−4] together with theoretical analyses of the observed band patterns,[5−10] have yielded a clear picture of how water networks are deformed when they attach to small anions.[11,12] Among the simplest of these systems is the hydrated halide series, $X^-\cdot(H_2O)_n$, (X = F, Cl, Br, I),[13−16] where the shapes of the larger clusters are driven by the asymmetric, single ionic H-bonding (SIHB) arrangement adopted by the binary $X^-\cdot H_2O$ complexes. In the larger halides, for example, the dangling hydrogen atoms of SIHB water molecules in the primary hydration shell form cyclic interwater networks in the minimum-energy structures.[13−15] Here we examine the evolution of the hydration motifs when a second chlorine atom is added to Cl^- to form the Cl_2^- diatomic species. This provides us with an opportunity to follow how a more extended electron distribution with similar orbital parentage (i.e., delocalization over the 3p orbitals of the chlorine atoms) affects the binary ion−molecule interaction as well as the morphologies of the higher hydrates.

On the basis of previous studies of diatomic anion hydration,[17,18] we anticipate that the shape of the excess electron distribution in Cl_2^- will be a determining factor in the structures adopted by the attached water networks. The X $^2\Sigma_u^+$ ground electronic state of Cl_2^- features a cylindrically symmetric, (orbitally) nondegenerate charge distribution most like that of the previously studied X $^3\Sigma^-$ state of NO^- (as opposed to the X $^2\Pi_g$ state of O_2^-). In the NO^- case, the binary $NO^-\cdot H_2O$ complex maintains the SIHB motif, with larger hydrates displaying interwater networking and cyclic structures.[18] The trihydrate provided a particularly distinct spectral signature of the structure, where the degenerate ring modes of the C_3-symmetry $(H_2O)_3$ subcluster are split, forming an evenly spaced triplet when the cyclic trimer attaches to the long axis of the cylindrical charge distribution in the $NO^-\cdot(H_2O)_3$ complex. One important difference introduced in the Cl_2^- species (relative to first-row anions such as NO^-) is its relatively long interatomic distance (1.27 Å vs 2.48 Å in NO^- and Cl_2^-, respectively).[19,20] This is relevant because we have recently shown this distance to be a critical parameter controlling the propensity for a water molecule to bind symmetrically to triatomic anions (i.e., with each hydrogen bound to an oxygen atom in XO_2^- anionic domains).[21] On the basis of this trend, we anticipate that the binary $Cl_2^-\cdot H_2O$ interaction will favor the symmetrical double ionic H-bonding (DIHB) arrangement, raising the interesting question of how subsequent water molecules will be accommodated. For example, binding a second water molecule to the ion in a symmetrical fashion would come at the expense of interwater networking, whereas the formation of an interwater bond like that in the $NO^-\cdot(H_2O)_2$ complex would require changing the binding motif of the water molecule initially attached to the ion from double to single ionic H-bonding.

To elucidate the structures of the $Cl_2^-\cdot(H_2O)_n$ clusters, we report the vibrational predissociation spectra of the argon-solvated species in the OH stretching region. Previous application of this method to the $Cl^-\cdot H_2O$ complex provided a clear signature of its asymmetric structure.[13] The SIHB arrangement in $Cl^-\cdot H_2O$ results in a characteristic pattern in the OH stretching vibrational spectrum as illustrated in Figure 1a.[4] The two OH stretch fundamentals are dramatically split into a strongly red-shifted band for the ionic H-bonded (IHB) hydrogen and a weaker free OH feature (F) very close to the centroid (3707 cm^{-1})[22] of the bands in the isolated water molecule. The two bands with intermediate intensity, appearing just above the strong OH_{IHB} transition, are due to the intramolecular bending overtone (B) and an ion−molecule stretching combination band (IM), respectively. The symmetrical binding motif has recently been observed in several triatomic systems (e.g., $CS_2^-\cdot H_2O$ and $SO_2^-\cdot H_2O$),[21,23] and in these cases, the OH stretches remain coupled but the red shift is dramatically reduced compared to that typically observed in the SIHB arrangement. The splitting between the coupled stretching modes of a DIHB water molecule is generally reduced relative to their separation in isolated water (~100 cm^{-1}), and the spectra of the complexes are dominated by the symmetric stretching fundamentals. This intensity distribution is likely a consequence of the fact that the dipole derivative associated with the υ_S vibration lies along

---

* Corresponding author. E-mail: mark.johnson@yale.edu.

10.1021/jp031239f CCC: $27.50

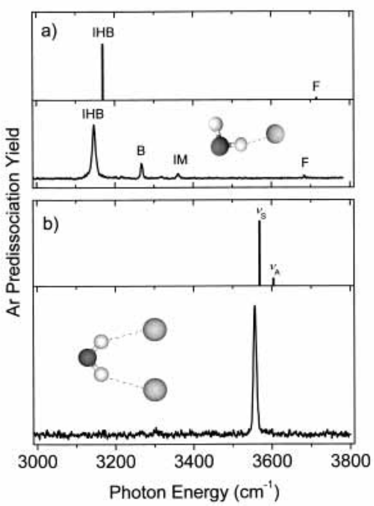

Figure 1. Calculated (top) and Ar predissociation IR (bottom) spectra of Cl^- and Cl_2^- monohydrates: (a) $Cl^-\cdot(H_2O)\cdot Ar_{11}$ and (b) $Cl_2^-\cdot(H_2O)\cdot Ar_3$. The spectrum of $Cl^-\cdot(H_2O)\cdot Ar_{11}$ has been previously reported.[4] The B3LYP/aug-cc-pVDZ harmonic fundamentals have been scaled by 0.9627, and letters denote band assignments (F = free OH stretch, IM = ion−molecule stretching combination band, B = intramolecular bending overtone, and IHB = ionic H-bonded OH stretch). υ_S and υ_A in b denote the symmetric and asymmetric OH stretching normal modes, respectively. Optimized geometries corresponding to the calculated spectra are included.

the ion−molecule axis, whereas that of the asymmetric stretch is perpendicular to it.

II. Experimental Section

The $Cl_2^-\cdot(H_2O)_n\cdot Ar_m$ clusters central to this study were created with a supersonic entrainment cluster ion source[3] and were characterized in the OH stretching region of the infrared using a double-focusing, tandem time-of-flight photofragmentation mass spectrometer.[24] Water vapor and dilute Cl_2 gas (1% in helium) were introduced via independent pulsed valves on the low-pressure side of an electron-beam ionized argon expansion.[3] Mass-selected clusters were irradiated with the mid-IR output from a Nd:YAG pumped OPO/OPA (LaserVision) laser source. This laser is tunable over the range of 2400−4500 cm^{-1} with a bandwidth of 2 cm^{-1} and an absolute wavenumber accuracy of about ±5 cm^{-1}. The reported spectra result from the addition of approximately 20 individual scans and are corrected for laser-pulse energy changes over the scan range.

III. Results and Discussion

III.A.1. Symmetrical Binding in the Monohydrate. The argon predissociation spectra of the $Cl^-\cdot H_2O$ and $Cl_2^-\cdot H_2O$ binary complexes are compared in Figure 1. The $Cl_2^-\cdot H_2O\cdot Ar_3$ spectrum obtained in this work is presented in the lower trace (Figure 1b) and is both very simple and dramatically different than that observed for $Cl^-\cdot H_2O$. The dichloride monohydrate spectrum consists of a single sharp feature located at 3556 cm^{-1}, over 400 cm^{-1} higher in energy than the OH_{IHB} transition in $Cl^-\cdot H_2O$. The absence of a free OH band indicates that both hydrogen atoms are bound to the ion in the DIHB motif. The behavior of $Cl_2^-\cdot H_2O$ is interesting in that, despite the fact that $Cl^-\cdot H_2O$ is very strongly bound and asymmetric, the $Cl_2^-\cdot H_2O$ transition displays the weakest red shift of any DIHB complex observed to date.[21,23,25]

Because we are not aware of previous theoretical work on the $Cl_2^-\cdot H_2O$ system, we carried out preliminary calculations at the B3LYP/aug-cc-pVDZ and MP2/aug-cc-pVDZ levels of theory to establish the likely solvation landscapes at play. All calculations reported here were made using the Gaussian 98 suite of programs,[26] and a summary of the calculations is presented in Table 1. The minimum-energy (B3LYP) structure recovered for $Cl_2^-\cdot H_2O$ is included in Figure 1b and indeed displays the symmetrical C_{2v} DIHB binding motif. The stick spectrum in Figure 1b indicates the calculated symmetric (υ_S) and asymmetric (υ_A) OH fundamentals, scaled by 0.9627 to correct approximately for anharmonicity at this level of theory. As expected, the symmetric stretch transition dominates the oscillator strength in this region, with the weaker asymmetric stretch lying closely (~40 cm^{-1}) above it. Similarly calculated fundamentals for the $Cl^-\cdot H_2O$ complex are also included in Figure 1a, confirming that the behavior of the smaller complex is also recovered at this level of theory.

TABLE 1: B3LYP/aug-cc-pVDZ Energies (hartrees) of $Cl_2^-\cdot(H_2O)_n$ Isomers

cluster	structure	H-bonding motif	energy
$Cl_2^-\cdot(H_2O)_1$	1-I	DIHB	−996.9790780
$Cl_2^-\cdot(H_2O)_2$	2-I	DIHB	−1073.4410880[a]
	2-II	DIHB	−1073.4399199[b]
$Cl_2^-\cdot(H_2O)_3$	3-I	SIHB	−1149.9048635
	3-II	DIHB	−1149.8987716
$Cl_2^-\cdot(H_2O)_4$	4-I	SIHB	−1226.3701272
	4-II	SIHB/DIHB	−1226.3631898
$Cl_2^-\cdot(H_2O)_5$	5-I	SIHB/DIHB	−1302.8277913
	5-II	SIHB	−1302.8316040

[a] After zero-point energy correction: −1073.3921009 hartrees. [b] After zero-point energy correction: −1073.3919452 hartrees.

III.A.2. Internal Energy Effects: Red Shifting of the OH Stretching Bands. One of the important aspects in the exploration of the potential surface for the hydrate is to follow how the spectra change with increasing internal energy. To assess this behavior qualitatively, one can compare the predissociation spectra of the bare and argon-solvated complexes, as the stronger binding energy of H_2O compared to that of Ar enables the bare complex to retain much more internal energy in the evaporative ensemble.[27] Figure 2 reproduces the argon predissociation spectrum of $Cl_2^-\cdot H_2O\cdot Ar_3$ (gray) along with the spectrum obtained by predissociation of the water molecule from $Cl_2^-\cdot H_2O$ (black). The spectrum of the bare complex is broader than that obtained by argon predissociation, as expected. But surprisingly, most of the oscillator strength in the warmer ensemble falls below the sharp feature arising from the cold complex. This red-shifting behavior warrants consideration because it opposes the trend established by the SIHB complexes (such as iodides),[28] where the warm complexes display a blue shift.

To understand the physical processes that govern the direction of the internal energy-induced band shifts for each class of complex, it is useful to invoke a vibrationally adiabatic picture. In this approach, we envision separate potential energy surfaces governing the soft-mode, ion−molecule (IM) displacements for each of the high-frequency OH stretching vibrational levels. In an SIHB complex, the ion−molecule stretching degree of freedom is typically more strongly bound in the $\upsilon = 1$ level of the OH stretch compared to that in $\upsilon = 0$.[29−32] This, in turn, results in an increase in the IM frequency for $\upsilon(OH) = 1$ relative to that for $\upsilon(OH) = 0$. When the IM levels become excited as the complex is warmed, the OH_{IHB} transition is thus blue degraded by the associated $\Delta\upsilon = 0$ sequence band structure involving the IM hot bands.

However, in the case of a DIHB complex such as $Cl_2^-\cdot H_2O$, the motion that most strongly changes with OH stretching

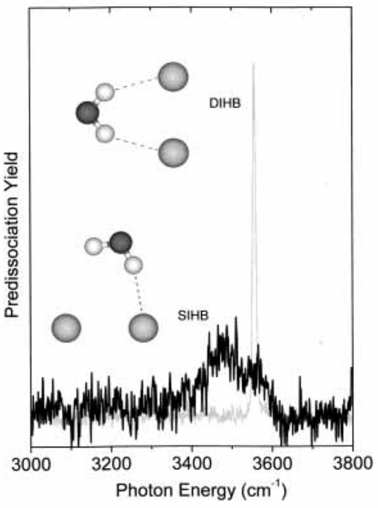

Figure 2. Predissociation spectra of $Cl_2^-{\cdot}H_2O{\cdot}Ar_3$ (gray) and $Cl_2^-{\cdot}H_2O$ (black). In the spectrum of the warmer bare complex (black), excitation of the water rocking soft mode causes a change in geometry toward the SIHB motif with an associated red shift.

excitation is the water rocking soft mode. This motion is, in fact, the displacement that mediates the conversion of the complex between DIHB and SIHB forms. This effect has been discussed at length in recent reports analyzing strong anharmonicity effects in the $CH_3NO_2^-{\cdot}H_2O$ and $CH_3CO_2^-{\cdot}H_2O$ systems.[21,25] The basic conclusion was that because the red shifts associated with SIHB geometries are much larger than those found at the DIHB structure, the adiabatic potential for the (~70 cm^{-1}) rocking motion is dramatically softened in the v(OH) = 1 level. In the case of the methylated anions, this anharmonic coupling causes a *change in the geometry* of the complex from the DIHB arrangement in the v(OH) = 0 stretching level to the SIHB structure in v(OH) = 1. This vibration-induced structure change thus explains the observed extended progression in the rocking mode upon excitation of the (cold) ground-state complex.

In the $Cl_2^-{\cdot}H_2O$ case, the anharmonic effects are much smaller than in $CH_3CO_2^-{\cdot}H_2O$, as evidenced by the absence of such soft-mode activity in the spectrum of the cold complex. However, the red degrading of the OH_{IHB} band upon warming is readily understood in the context of a softer potential for the rocking mode in the v(OH) = 1 stretching level, which lowers the frequency of the IM mode in the adiabatic state arising from OH(v = 1). This scenario is illustrated by the structures in Figure 2, where the (warmer) bare complex explores the asymmetric SIHB arrangement, displacing the spectrum to lower energy with internal excitation.

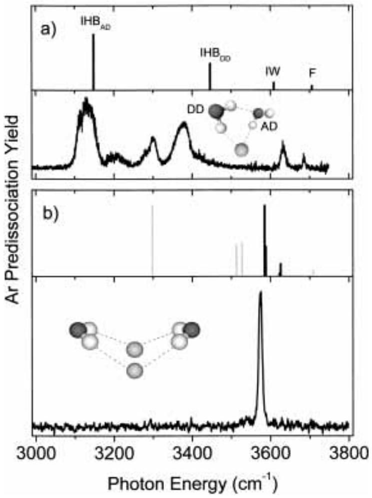

Figure 3. Calculated (top) and Ar predissociation IR (bottom) spectra of Cl^- and Cl_2^- dihydrates: (a) $Cl^-{\cdot}(H_2O)_2{\cdot}Ar_3$ and (b) $Cl_2^-{\cdot}(H_2O)_2{\cdot}Ar$. The spectrum of $Cl^-{\cdot}(H_2O)_2{\cdot}Ar_3$ has been previously reported.[14] The B3LYP/aug-cc-pVDZ harmonic fundamentals have been scaled by 0.9627, and letters denote band assignments (F = free OH stretch, IW = interwater H-bonded OH stretch, IHB_{DD} = ionic H-bonded OH stretch on a double-donor water molecule, and IHB_{AD} = ionic H-bonded OH stretch on an acceptor/donor water molecule). Optimized geometries corresponding to the calculated spectra are included. For $Cl_2^-{\cdot}(H_2O)_2$, frequencies are shown for two geometries shown in Figure 4: 2-I (gray) and 2-II (black).

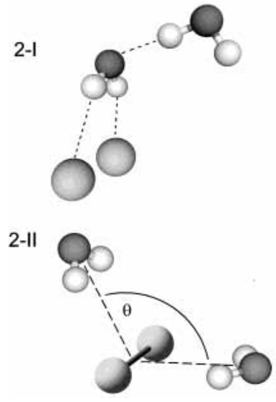

Figure 4. Optimized geometries of $Cl_2^-{\cdot}(H_2O)_2$ at the B3LYP/aug-cc-pVDZ level.

III.B. Dihydrate: Attachment of Two Water Molecules with the Binary (DIHB) Motif. Figure 3 presents a comparison of the Cl^- and Cl_2^- dihydrates. The $Cl^-{\cdot}(H_2O)_2$ spectrum shown in the upper trace has been reported previously,[14] whereas the lower trace presents the $Cl_2^-{\cdot}(H_2O)_2$ spectrum obtained in this work. The $Cl^-{\cdot}(H_2O)_2$ complex displays the expected pattern of bands when an intact water dimer attaches to an anion with each water molecule binding in an SIHB motif, as depicted in the inset. The addition of a second chlorine atom results in a dramatic simplification of the dihydrate spectrum, which is again dominated by a single sharp line. In fact, the $Cl_2^-{\cdot}(H_2O)_2$ spectrum appears remarkably similar to that of $Cl_2^-{\cdot}H_2O$, with the sharp line appearing only 18 cm^{-1} above the line observed in the monohydrate. This is the most remarkable result of the present study because it immediately suggests that rather than binding to each other, the two water molecules attach more or less independently to the ion, each with the DIHB motif established in the binary complex!

Because the binding motif suggested by the spectra is unusual, we have extended the (B3LYP/aug-cc-pVDZ and MP2/aug-cc-pVDZ) calculations to the dihydrate to investigate the possibility that two water molecules bind to the ion in the DIHB arrangement. Interestingly, the lowest-energy form that we found (labeled 2-I in Figure 4) features a networked water dimer bound to the ion. In this structure, a second water molecule simply H-bonds to the first (rather than the ion), and the molecule in primary coordination retains its DIHB motif. The overall situation is reminiscent of that found previously in the $I^-{\cdot}(MeOH)_2$ cluster, where this intersolvent H-bonded structure was, in fact, consistent with the observed spectrum.[33] In the $Cl_2^-{\cdot}(H_2O)_2$ case, however, the calculated spectrum associated with the 2-I structure, indicated by the gray lines in Figure 3b, is not consistent with the singular feature in the observed spectrum.

Additional calculations reveal that the hydration topology of the dihydrate is rather complicated despite the simplicity of the observed spectrum. Several other low-lying isomers were recovered at the B3LYP level of theory, such as cyclic structures where a water dimer binds to both chlorine atoms (such as those found in $O_2^- \cdot (H_2O)_2$ and $NO^- \cdot (H_2O)_2$),[12,17,18] but these again yield complex, multiline spectra at odds with the observed feature. Motivated by the spectrum, we also initiated a calculation with both water molecules in the DIHB motif and all atoms lying in a plane, which evolved to the local minimum (structure 2-II) displayed in Figure 4. Isomer 2-II features both water molecules bound to Cl_2^- in the DIHB motif, with a dihedral angle (denoted θ in Figure 4) of 135° (MP2 yields 115°) between the two water molecules. The planar D_{2h} structure ($\theta = 180°$ between the DIHB waters) was found to be a first-order saddle point. Structure 2-II is calculated to occur 256 cm^{-1} (B3LYP) above structure 2-I, but when zero-point energies are taken into account, this energy is reduced to 34 cm^{-1} and it is the isomer closest in energy to that of 2-I.

The calculated (B3LYP, scaled) fundamentals for isomer 2-II are indicated by the black lines in Figure 3b and are in much better agreement with the observed spectrum than the transitions calculated for isomer I. The position of the strong feature is very well recovered, and on this basis, we attribute the dominant feature to an unresolved doublet involving the in-phase and out-of-phase symmetric stretching vibrations on each water molecule. We therefore conclude that the structure responsible for the observed spectrum is most probably isomer 2-II, and as with the monohydrate, the calculations overestimate the intensity of the weaker feature on the high-energy side derived from the asymmetric OH stretches on the constituent water molecules. It would be valuable to explore these structures at higher levels of theory to clarify the relative energies of the various isomers, as at present is seems that the observed structure results from preferential formation of a higher-energy form, presumably due to the kinetics of the ion source.

It is important to emphasize that isomer 2-II is a very unusual arrangement for anionic hydration. All of the dihydrates observed to date occur with an intact water dimer subcluster like that found in $Cl^- \cdot (H_2O)_2$ (inset in Figure 3a). It is true that very strongly basic anions (such as F^- and OH^-) have been observed to break up the water dimer,[11,14] but these occur with both water molecules attached to the ion in an SIHB configuration. In those cases, the ion-induced dissociation of the water dimer has been traced to the three-body repulsion between the water molecules, which occurs when a very strong binary interaction explores charge-transfer electronic configurations (e.g., $F^- \cdot H_2O \rightarrow HF + OH^-$) and thus builds up negative charge on the water molecule. The $Cl_2^- \cdot (H_2O)_2$ case does not correspond to this regime because the symmetrical binary interaction is rather weak and displays a very modest red shift.

III.C. Higher Hydrates: Emergence of the Cyclic Water Networks. Figure 5 presents an overview of the predissociation spectra obtained for all of the hydrates studied here, $Cl_2^- \cdot (H_2O)_{1-5}$, as well as the anharmonicity-corrected frequencies (the B3LYP/aug-cc-pVDZ level) for various structures calculated to be locally stable. Whereas the $Cl_2^- \cdot (H_2O)_{1-2}$ complexes exhibited only one infrared feature in the 3000−3800-cm^{-1} region, there are at least six distinct absorption bands for $Cl_2^- \cdot (H_2O)_3$, and similarly complex spectra are observed for $Cl_2^- \cdot (H_2O)_{4-5}$. The presence of this complexity indicates that a variety of hydrogen bonding environments are at play, in contrast to the highly symmetrical ionic H-bonding motif presented in the mono- and dihydrates.

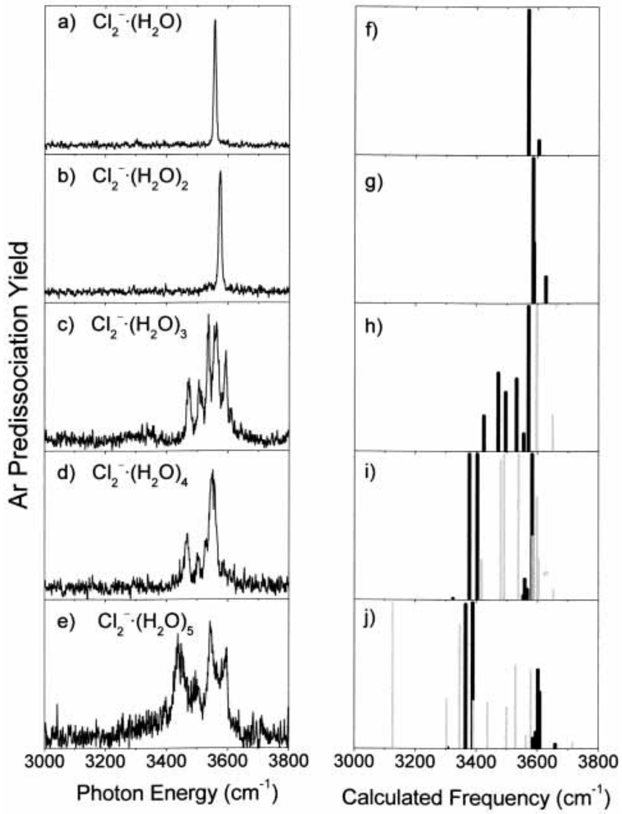

Figure 5. Ar predissociation spectra of (a) $Cl_2^- \cdot H_2O \cdot Ar_3$, (b) $Cl_2^- \cdot (H_2O)_2 \cdot Ar$, (c) $Cl_2^- \cdot (H_2O)_3 \cdot Ar_2$, (d) $Cl_2^- \cdot (H_2O)_4 \cdot Ar$, and (e) $Cl_2^- \cdot (H_2O)_5 \cdot Ar$ and calculated IR spectra of (f) $Cl_2^- \cdot (H_2O)$, (g) $Cl_2^- \cdot (H_2O)_2$, (h) $Cl_2^- \cdot (H_2O)_3$, (i) $Cl_2^- \cdot (H_2O)_4$, and (j) $Cl_2^- \cdot (H_2O)_5$. The B3LYP/aug-cc-pVDZ harmonic fundamentals have been scaled by 0.9627. For $Cl_2^- \cdot (H_2O)_n$ ($n = 3-5$), calculated fundamentals are displayed for the two isomers indicated in Figure 7, denoted by n-I (black) and n-II (gray).

Although it is not our goal to elucidate the precise structures of the larger hydrates, there are a few features in the trend that warrant discussion. Focusing on the trihydrate, it is again valuable to consider the dichloride behavior in the context of other ions studied previously. In Figure 6, we present the spectra of $Cl^- \cdot (H_2O)_3$, $I^- \cdot (H_2O)_3$, and the $Cl_2^- \cdot (H_2O)_{3-5}$ systems obtained here. The monatomic halides feature a C_3-symmetry water trimer subcluster, with three hydrogens attached to the ion (labeled IHB) and the other three involved in the cyclic trimer network (labeled Ring). In the most strongly bound $Cl^- \cdot (H_2O)_3$ system, these two classes of OH stretching bands are split far apart, with the IHB bands lying well below the ring modes, which appear with a characteristic 2:1 intensity pattern. These two classes of bands are brought closer together in the more weakly bound $I^- \cdot (H_2O)_3$ system, an effect traced to the strengthening of the ring as the H-bond to the ion is weakened in the larger halide. The clump of bands observed for $Cl_2^- \cdot (H_2O)_3$ falls between these two sets of bands in $I^- \cdot (H_2O)_3$, and the absence of the 2:1 band pattern immediately signals that this trimer does not form to one of the chlorine atoms along the bond axis of Cl_2^- (which would have C_3 symmetry). Rather, it appears that the trimer either breaks apart or attaches to the side of the Cl_2^- intermolecular axis, as was found to be the case in $NO^- \cdot (H_2O)_3$.[18] With this behavior in mind, it is most interesting that the $Cl_2^- \cdot (H_2O)_4$ and $Cl_2^- \cdot (H_2O)_5$ spectra again split into two clumps of bands, with the $n = 5$ complex displaying a larger spread than that of $n = 4$.

To understand qualitatively the likely morphologies at play, we turn to the calculated structures presented in Figure 7 and

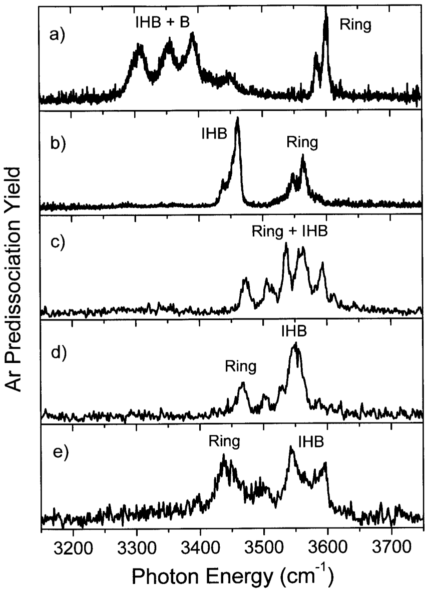

Figure 6. Ar predissociation spectra of (a) $Cl^-\cdot(H_2O)_3\cdot Ar_3$, (b) $I^-\cdot(H_2O)_3\cdot Ar_3$, (c) $Cl_2^-\cdot(H_2O)_3\cdot Ar_2$, (d) $Cl_2^-\cdot(H_2O)_4\cdot Ar$, and (e) $Cl_2^-\cdot(H_2O)_5\cdot Ar$. Bands are assigned to normal modes predominantly involving IHB and ring OH stretches, in addition to the extra bands due to a Fermi-type interaction with the (0−2) intramolecular bending overtones (B) of the water molecules.

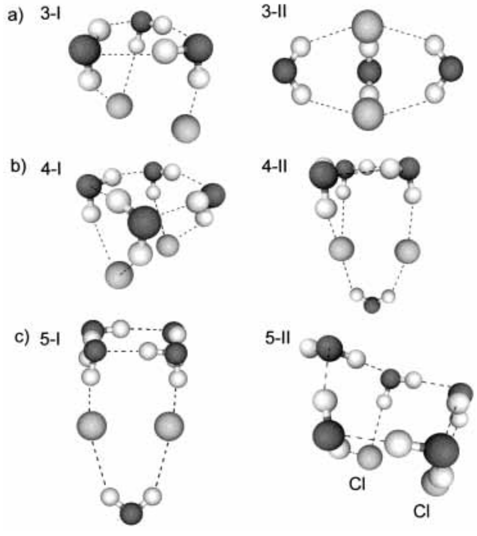

Figure 7. Calculated structures of $Cl_2^-\cdot(H_2O)_{3-5}$ optimized at the B3LYP/aug-cc-pVDZ level: (a) $Cl_2^-\cdot(H_2O)_3$, (b) $Cl_2^-\cdot(H_2O)_4$, and (c) $Cl_2^-\cdot(H_2O)_5$.

the associated (calculated, B3LYP/aug-cc-pVDZ) spectra shown in the right panel of Figure 5. Our major conclusion from this exercise is that the Cl_2^- hydrates present an interesting case where the IHB and ring stretches effectively "cross over" such that the ring modes fall below the IHB bands in the tetrahydrate. The overall scenario is that the two classes of bands accidentally fall quite close together in the trihydrate, leading to a congested set of bands in which the two local oscillators (ion and interwater H-bonded) are heavily mixed.

More specifically, the calculations indeed identify a locally stable D_{3h} isomeric form (labeled 3-II) for the trihydrate indicated in Figure 7a, but it is quite high in energy, lying about 1300 cm^{-1} above the minimum-energy form (3-I). Moreover, the calculated spectrum of the D_{3h} form (gray bars in Figure 5h) is very simple, like those of the related $n = 1$ and 2 complexes, whereas the lower-energy form (3-I) gives rise to six closely spaced bands similar to that observed. We therefore conclude that the trihydrate adopts the distorted cyclic network structure, similar to that observed in $NO^-\cdot(H_2O)_3$.[18] Note that this "sideways" attached trimer accommodates all three water molecules in the SIHB motif, indicating that the interwater network formation has overcome the tendency of the individual water molecules to attach in the DIHB arrangement.

The assignment of structures for the $n = 4$ and 5 clusters is not conclusive. Two low-lying forms were recovered for each as indicated in Figure 7b and c, which were motivated by initial guesses based on intuition. For $n = 4$, these are the expected cyclic tetramer subcluster ("4 + 0") and the "3+1" form (3 SIHB + 1 DIHB water molecules), which is a hydrid of the $n = 3$ and 1 motifs and is found to be about 1500 cm^{-1} higher in energy. The observed $n = 4$ spectrum is in the best agreement with the 4 + 0 structure, but the calculations overestimate the splitting. In either case, however, the ring modes are calculated to fall below the IHB bands as discussed above.

For $n = 5$, calculations indicate that the cyclic pentamer and a hybrid 4 + 1 type structure at higher energy are locally stable, by analogy to the situation for $n = 4$. Of these two, we find the best agreement with the calculated spectrum for the higher-energy 4 + 1 form because the cyclic pentamer subcluster should display a very red-shifted transition, which is not observed. Again, the ring modes of both isomers lie below the IHB bands, and the observed spectrum indeed extends farther to the blue than that of $n = 4$, possibly reflecting a weaker interaction with the ion as the number of attached water molecule increases.[34]

IV. Summary

Vibrational predissociation spectroscopy of the $Cl_2^-\cdot(H_2O)_n$ clusters in the OH stretching region indicates that the $Cl_2^-\cdot H_2O$ binary interaction occurs with each hydrogen atom attached to a chlorine atom in a double ionic H-bond motif (DIHB). This motif is maintained upon the addition of the second water molecule, and water networks begin to form in the $n \geq 3$ clusters. The OH stretching bands displayed by the larger hydrates are complicated by the fact that the ionic H-bonded OH stretching bands lie very close to the interwater fundamentals, and calculations suggest that for $n \geq 4$ the interwater network vibrations may, in fact, fall below the ionic H-bonds in this weakly bound system.

Acknowledgment. We gratefully thank the National Science Foundation for supporting this work.

References and Notes

(1) Johnson, M. S.; Kuwata, K. T.; Wong, C.-K.; Okumura, M. *Chem. Phys. Lett.* **1996**, *260*, 551.

(2) Ayotte, P.; Weddle, G. H.; Kim, J.; Johnson, M. A. *Chem. Phys.* **1998**, *239*, 485.

(3) Robertson, W. H.; Kelley, J. A.; Johnson, M. A. *Rev. Sci. Instrum.* **2000**, *71*, 4431.

(4) Corcelli, S. A.; Kelley, J. A.; Tully, J. C.; Johnson, M. A. *J. Phys. Chem. A* **2002**, *106*, 4872.

(5) Irle, S.; Bowman, J. M. *J. Chem. Phys.* **2000**, *113*, 8401.

(6) Robertson, W. H.; Johnson, M. A.; Myshakin, E. M.; Jordan, K. D. *J. Phys. Chem. A* **2002**, *106*, 10010.

(7) Baik, J.; Kim, J.; Majumdar, D.; Kim, K. S. *J. Chem. Phys.* **1999**, *110*, 9116.

(8) Weber, J. M.; Robertson, W. H.; Johnson, M. A. *J. Chem. Phys.* **2001**, *115*, 10718.

(9) Chaban, G. M.; Jung, J. O.; Gerber, R. B. *J. Phys. Chem. A* **2000**, *104*, 2772.

(10) Xantheas, S. S. *J. Phys. Chem.* **1996**, *100*, 9703.

(11) Robertson, W. H.; Diken, E. G.; Price, E. A.; Shin, J.-W.; Johnson, M. A. *Science* **2003**, *299*, 1367.

(12) Weber, J. M.; Kelley, J. A.; Nielsen, S. B.; Ayotte, P.; Johnson, M. A. *Science* 2**000**, *287*, 2461.

(13) Ayotte, P.; Weddle, G. H.; Kim, J.; Johnson, M. A. *J. Am. Chem. Soc.* **1998**, *120*, 12361.

(14) Ayotte, P.; Nielsen, S. B.; Weddle, G. H.; Johnson, M. A.; Xantheas, S. S. *J. Phys. Chem. A* **1999**, *103*, 10665.

(15) Ayotte, P.; Weddle, G. H.; Johnson, M. A. *J. Chem. Phys.* **1999**, *110*, 7129.

(16) Ayotte, P.; Kelley, J. A.; Nielsen, S. B.; Johnson, M. A. *Chem. Phys. Lett.* **2000**, *316*, 455.

(17) Weber, J. M.; Kelley, J. A.; Robertson, W. H.; Johnson, M. A. *J. Chem. Phys.* **2001**, *114*, 2698.

(18) Myshakin, E. M.; Jordan, K. D.; Robertson, W. H.; Weddle, G. H.; Johnson, M. A. *J. Chem. Phys.* **2003**, *118*, 4945.

(19) Travers, M. J.; Cowles, D. C.; Ellison, G. B. *Chem. Phys. Lett.* **1989**, *164*, 449.

(20) Sullivan, S. A.; Freiser, B. S.; Beauchamp, J. L. *Chem. Phys. Lett.* **1977**, *48*, 294.

(21) Robertson, W. H.; Price, E. A.; Weber, J. M.; Shin, J.-W.; Weddle, G. H.; Johnson, M. A. *J. Phys. Chem. A* **2003**, *107*, 6527.

(22) Shimanouchi, T. Molecular Vibrational Frequencies. In *NIST Chemistry WebBook*; Mallard, W. G., Linstrom, P. J., Eds.; National Institute of Standards and Technology (http://webbook.nist.gov): Gaithersburg, MD, 1998; Vol. 69.

(23) Woronowicz, E. A.; Robertson, W. H.; Weddle, G. H.; Johnson, M. A.; Myshakin, E. M.; Jordan, K. D. *J. Phys. Chem. A* **2002**, *106*, 7086.

(24) Johnson, M. A.; Lineberger, W. C. *Techniques for the Study of Gas-Phase Ion Molecule Reactions*; Wiley: New York, 1988; p 591.

(25) Myshakin, E. M.; Jordan, K. D.; Sibert, E. L., III; Johnson, M. A. *J. Chem. Phys.* **2003**, *119*, 10138.

(26) Frisch, M. J.; Trucks, G. W.; Schlegel, H. B.; Scuseria, G. E.; Robb, M. A.; Cheeseman, J. R.; Zakrzewski, V. G.; Montgomery, J. A., Jr.; Stratmann, R. E.; Burant, J. C.; Dapprich, S.; Millam, J. M.; Daniels, A. D.; Kudin, K. N.; Strain, M. C.; Farkas, O.; Tomasi, J.; Barone, V.; Cossi, M.; Cammi, R.; Mennucci, B.; Pomelli, C.; Adamo, C.; Clifford, S.; Ochterski, J.; Petersson, G. A.; Ayala, P. Y.; Cui, Q.; Morokuma, K.; Malick, D. K.; Rabuck, A. D.; Raghavachari, K.; Foresman, J. B.; Cioslowski, J.; Ortiz, J. V.; Stefanov, B. B.; Liu, G.; Liashenko, A.; Piskorz, P.; Komaromi, I.; Gomperts, R.; Martin, R. L.; Fox, D. J.; Keith, T.; Al-Laham, M. A.; Peng, C. Y.; Nanayakkara, A.; Gonzalez, C.; Challacombe, M.; Gill, P. M. W.; Johnson, B. G.; Chen, W.; Wong, M. W.; Andres, J. L.; Head-Gordon, M.; Replogle, E. S.; Pople, J. A. *Gaussian 98*; Gaussian, Inc.: Pittsburgh, PA, 1998.

(27) Klots, C. E. *J. Chem. Phys.* **1985**, *83*, 5854.

(28) Nielsen, S. B.; Ayotte, P.; Kelley, J. A.; Johnson, M. A. *J. Chem. Phys.* **1999**, *111*, 9593.

(29) Weiser, P. S.; Wild, D. A.; Bieske, E. J. *J. Chem. Phys.* **1999**, *110*, 9443.

(30) Weiser, P. S.; Wild, D. A.; Bieske, E. J. *Chem. Phys. Lett.* **1999**, *299*, 303.

(31) Wild, D. A.; Milley, P. J.; Loh, Z. M.; Wolynec, P. P.; Weiser, P. S.; Bieske, E. J. *J. Chem. Phys.* **2000**, *113*, 1075.

(32) Wild, D. A.; Loh, Z. M.; Wolynec, P. P.; Weiser, P. S.; Bieske, E. J. *Chem. Phys. Lett.* **2000**, *332*, 531.

(33) Robertson, W. H.; Karapetian, K.; Ayotte, P.; Jordan, K. D.; Johnson, M. A. *J. Chem. Phys.* **2002**, *116*, 4853.

(34) Choi, J.-H.; Kuwata, K. T.; Cao, Y.-B.; Okumura, M. *J. Phys. Chem. A* **1998**, *102*, 503.